

Directly Measuring Material Proportions Using Hyperspectral Compressive Sensing

Alina Zare, *Member, IEEE*, Paul Gader, *Fellow, IEEE*, and Karthik S. Gurumoorthy

Abstract—A compressive sensing framework is described for hyperspectral imaging. It is based on the widely used linear mixing model, *LMM*, which represents hyperspectral pixels as convex combinations of small numbers of endmember (material) spectra. The coefficients of the endmembers for each pixel are called proportions. The endmembers and proportions are often the sought after quantities; the full image is an intermediate representation used to calculate them. Here a method for estimating proportions and endmembers directly from compressively sensed hyperspectral data based on *LMM* is shown. Consequently, proportions and endmembers can be calculated directly from compressively sensed data with no need to reconstruct full hyperspectral images. If spectral information is required, endmembers can be reconstructed using compressive sensing reconstruction algorithms. Furthermore, given known endmembers, the proportions of the associated materials can be measured directly using a compressive sensing imaging device. This device would produce a multi-band image; the bands would directly represent the material proportions.

I. INTRODUCTION

A Hyperspectral image can be thought of as a three-dimensional array, $X(i, j, \lambda)$, of real values. The first two dimensions correspond to standard spatial coordinates and the third dimension corresponds to wavelength [1]. The values in the array generally correspond to the physical quantities of reflectance, radiance, or emissivity. Typical wavelength ranges include the Visible, Near-Infra-Red, Short-Wave IR, and Long-Wave IR. These wavelength ranges are imaged in tens or hundreds of narrow spectral bands. We will refer to the vector of values at each spatial location as a pixel, keeping in mind that these vectors range in dimensionality from tens to hundreds. Hyperspectral image analysis differs from standard gray-scale, color, or even multi-spectral image analysis by virtue of the fact that the major focus is on using spectral information at each pixel to detect the presence of materials in the imaged scene. For this reason, some prefer to refer to the process of imaging and analyzing hyperspectral images as *Imaging Spectroscopy* to highlight the analogy to the use of spectroscopy in chemistry. In chemistry, the fact that all atoms have characteristic spectral wavelengths at which they will emit photons can be used to determine the percentage of different materials in a substance. Many techniques are used in

chemistry labs to determine the relative percentage of different substances within a mixed substance.

Hyperspectral image analysis is based on loosely following the ideas from spectroscopy in chemistry. It is assumed that there are a small number of materials in the imaged scene that contribute to the spectral content measured at each pixel. The spectra of these materials are referred to as endmembers. In contrast to general chemistry, however, a hyperspectral imaging device cannot generally produce information at the atomic or molecular level. For example, there may be grass, soil, sidewalks, and leaves in a given scene. In imaging spectroscopy, those materials would be considered the basic substances, or endmembers, rather than the different types of atoms and molecules contained within the grasses. Consequently, the substances or materials that are identifiable in a hyperspectral scene are usually more complex and have complicated responses compared to laboratory spectroscopy.

There are a number of possible ways to model the assumption that the spectral vector at a particular pixel is a mixture of a small number of materials. The most common is the Linear Mixing Model which models each pixel as a convex combination of the endmember spectra. The model can be written $\mathbf{x}_i = \mathbf{E}\mathbf{p}_i$ where $\mathbf{x}_i \in \mathbb{R}^D$ is the spectrum at the i^{th} hyperspectral pixel, \mathbf{E} is a $D \times M$ matrix whose columns contain the endmembers in the data [1]. The j^{th} component of \mathbf{p}_i , denoted by p_{ij} , represents the proportion of the j^{th} endmember in the i^{th} pixel. The proportions for each pixel are constrained as in Equation 1.

$$p_{ij} \geq 0, \forall i, j \quad \text{and} \quad \sum_{i=1}^M p_{ij} = 1 \forall j \quad (1)$$

LMM holds for a spectral pixel \mathbf{x}_i with respect to an endmember matrix \mathbf{E} if there exist proportions \mathbf{p}_i such that $\mathbf{x}_i = \mathbf{E}\mathbf{p}_i$ i.e. if \mathbf{x}_i is in the simplex defined by \mathbf{E} where $\mathbf{x}_i = \mathbf{E}\mathbf{p}_i$, is called the *LMM Representation*. The symbols in *LMM* will be used consistently throughout this paper.

The term *Hyperspectral Unmixing*, or simply *Spectral Unmixing*, refers to any physical or computational realization of a process that decomposes an input hyperspectral scene into endmembers and proportions. The inputs to the proportion estimation process are: (1) a set of spectra, $\{\mathbf{e}_1, \mathbf{e}_2, \dots, \mathbf{e}_M\}$ representing endmembers, and (2) a set of spectra, $\{\mathbf{x}_1, \mathbf{x}_2, \dots, \mathbf{x}_N\}$, from a hyperspectral image. The outputs are: a set of M proportions for each pixel representing the fractions of the materials associated with the endmembers that appear in the pixel. The endmember detection problem, loosely defined, consists of finding a set of endmembers that somehow “best”

A. Zare is with the Department of Electrical and Computer Engineering, University of Missouri, Columbia, MO, 65211 USA e-mail: zarea@missouri.edu

P. Gader and K. Gurumoorthy are with the Department of Computer and Information Science and Engineering, University of Florida, Gainesville, FL, 32611 USA e-mail: pgader@cise.ufl.edu, ksg@cise.ufl.edu

Manuscript received December 10, 2010, revised May 27, 2011 and August 8, 2011, accepted August 31, 2011.

represent a the pixels in a hyperspectral image using the *LMM*. The union of the problems of endmember detection and proportion estimation is the problem of representing pixels in a hyperspectral image using the *LMM*. The problem is ill-posed since, for any finite set of spectra, there exist infinitely many sets of endmembers and proportions that can exactly represent all the spectra. Therefore regularization terms must be used. An enormous amount of research has been conducted in the area of hyperspectral unmixing and endmember detection [2–4]. It is noted that the *LMM* is the most common model. Piecewise linear and other nonlinear models are also under investigation but are not as well understood.

It is generally difficult to estimate a good *LMM* using D dimensions for many reasons, including (1) many bands are non-informative, either because they do not vary with the imaged materials or they are absorbed by the atmosphere, (2) mathematical approaches may require low-dimensionality for full rank matrices, or (3) numerical problems occur more easily in high dimensions. Therefore, it is common to reduce dimensionality using standard transforms such as Principal Components, Maximum Noise Fraction, or Hierarchical dimensionality reduction [5; 6]. Proportion estimation is performed using either a large endmember spectral library or in conjunction with an endmember detection algorithm. In either case, each pixel is assumed to be a convex combination of a small number of the large number of possible endmembers. Each pixel can be viewed as a sparse combination of the endmembers [7; 8]. The set of all possible endmembers forms the dictionary. Typical ranges of values are that the dimensionality D ranges from around 100 up to 250 whereas M ranges from about 3 to 20. Thus, the *LMM* offers a natural sparse representation in a basis that is physically meaningful and can be used directly for hyperspectral image analysis.

Compressive sensing has been investigated intensively recently. Briefly, the compressive sensing framework is as follows, signals, $\{\mathbf{x}^{(u)} \in \mathbb{R}^D\}$, are assumed to have a sparse representation with respect to a basis. Often, an original signal, $\mathbf{x}^{(u)}$, can be reconstructed from random projections, $\mathbf{x}^{(c)} = \mathbf{S}\mathbf{x}^{(u)}$ where the dimensionality of $\mathbf{x}^{(c)}$ is much lower than $\mathbf{x}^{(u)}$. The matrix \mathbf{S} is called the sensing matrix. Full descriptions are easily found [9–11]. Reconstructing $\mathbf{x}^{(u)}$ from $\mathbf{x}^{(c)}$ generally requires optimization such as a solving a linear program or minimizing an l_1 -penalized quadratic.

Sometimes reconstruction is required to produce an output suitable for a human, such as an image for viewing. However, here it is often the case that reconstruction is only an intermediate step in the process of computing other desired quantities. The *LMM* of hyperspectral images can obviate the need for reconstruction, because parameters of the *LMM* can be calculated directly from compressed data. Sensing a compressed version of a hyperspectral image, reconstructing it, estimating the parameters of the *LMM* to produce a representation in terms of a small number of endmembers is inefficient. In this paper, it is shown that there is no need to reconstruct the hyperspectral image to estimate the *LMM* model for a hyperspectral image.

More precisely, a traditionally sensed and processed hyperspectral image is acquired in D spectral bands, or dimensions,

then reduced to a smaller number of dimensions, and then further reduced to M dimensions using proportion estimation and endmember detection techniques where $M \ll D$ (e.g. M is 5 and D is 220). Using this common line of hyperspectral analysis, often the desired information are the proportion maps for a hyperspectral image which indicate the location and abundance of each material in the scene. The *LMM* representation (in M dimensions) contains the desired information and this fact implies that the decompression and dimensionality reduction steps are unnecessary. In this paper, it is shown that: (1) the desired information can be estimated as accurately from compressively sensed hyperspectral as from traditionally sensed hyperspectral data and (2) if the *LMM* holds, then the proportions of particular materials in each pixel can be measured directly with a compressive sensing imager. The approach is similar in spirit to that of Gurbuz et al. who showed that Hough transforms could be computed directly from compressively sensed images [12]

The development proceeds by first establishing notation and then developing items (1) and (2) in the previous paragraph. Suppose $\mathbf{X}^{(u)}$ is a matrix whose columns are (uncompressed) hyperspectral pixels, then $\mathbf{X}^{(u)} = \mathbf{E}^{(u)}\mathbf{P}$ where the columns of the matrix $\mathbf{E}^{(u)}$ are the true uncompressed endmember spectra and the columns of the matrix \mathbf{P} contain the true proportions associated with each hyperspectral pixel. Let \mathbf{S} denote a sensing matrix and $\mathbf{X}^{(c)} = \mathbf{S}\mathbf{X}^{(u)}$. Each column of $\mathbf{X}^{(c)}$ is a compressed pixel. The compressed data can be represented using the sensing matrix, endmembers and proportions as shown in Equation 2.

$$\mathbf{X}^{(c)} = \mathbf{S}\mathbf{X}^{(u)} = \mathbf{S}\mathbf{E}^{(u)}\mathbf{P} = \mathbf{E}^{(c)}\mathbf{P} \quad (2)$$

Hence, compressed pixels can be represented by a convex combination of the compressed endmembers, $\mathbf{E}^{(c)}$, weighted by their true proportions. Assume the dimensionality of the compressively sensed data, d , is greater than or equal to one less than the number of endmembers, $M - 1$, and that the endmembers are linearly independent. Consequently, if each element of \mathbf{S} is drawn randomly from a standard Normal distribution, then it is almost surely full-rank so the columns of $\mathbf{E}^{(c)}$ are almost surely linearly independent. Then, this implies that, given compressed endmembers, the proportions are uniquely determined and equal to the true proportions.

If the endmembers, $\mathbf{E}^{(u)}$, are known, then the endmembers that would result from compressive sensing can be computed, $\mathbf{E}^{(c)} = \mathbf{S}\mathbf{E}^{(u)}$. The proportions for each pixel can be computed directly from the compressed data, $\mathbf{X}^{(c)}$ using any unmixing algorithm that produces the correct set of proportions when the *LMM* holds for a pixel. As mentioned above, the proportions so obtained must be the same as those obtained directly from traditionally sensed hyperspectral data.

Furthermore, if $\mathbf{E}^{(c)}$ is known, then a sensing matrix can be designed in which the proportions are measured directly with the compressive sensing imager. In the case that the endmembers are unknown, then endmember detection and proportion estimation can be performed entirely in the compressed domain without the need to decompress the measured data. In Section II, computation of proportions on the compressed data given known endmembers is described. The effects of noise

are empirically evaluated using simulated data with increasing levels of noise. In Section III, the method of directly sensing the proportions using known endmembers is described. In Section IV, a method of estimating the endmembers given proportions on compressed data is described. These endmembers could be reconstructed using traditional compressive sensing techniques if knowledge of their spectral content is required. Combining the methods from Section II and Section IV, an iterative endmember detection and proportion estimation method is defined for compressively sensed hyperspectral data.

II. SPECTRAL UNMIXING ON COMPRESSIVELY SENSED DATA

Suppose that \mathbf{S} is a random $d \times D$ sensing matrix and that

$$\begin{aligned}\mathbf{X}^{(c)} &= \mathbf{S}\mathbf{X}^{(u)} \\ \mathbf{E}^{(c)} &= \mathbf{S}\mathbf{E}^{(u)}.\end{aligned}\quad (3)$$

Let U denote an unmixing algorithm that calculates exact answers when they exist. More specifically, let $\mathbf{X}^{(u)}$ be a $D \times N$ matrix of spectral pixels, and $\mathbf{E}^{(u)}$ be a $D \times M$ matrix of endmembers. If there exist proportions \mathbf{P} such that $\mathbf{X}^{(u)} = \mathbf{E}^{(u)}\mathbf{P}$ and if $U(\mathbf{X}^{(u)}, \mathbf{E}^{(u)}) = \tilde{\mathbf{P}}$, then $\tilde{\mathbf{P}} = \mathbf{P}$. In such a case it must be true that $U(\mathbf{X}^{(c)}, \mathbf{E}^{(c)}) = \mathbf{P}$. Hence, algorithm U will calculate the correct answer directly from the compressively sensed data.

Moreover, if algorithm U generates proportions that minimize the sum of the squared errors (SSE), i.e. if

$$U(\mathbf{X}^{(c)}, \mathbf{E}^{(c)}) = \min_{\mathbf{P}} \|\mathbf{X}^{(u)} - \mathbf{E}^{(u)}\mathbf{P}\|_2^2 \quad (4)$$

subject to the constraints in Equation 1, then, even if the minimum SSE is not zero, U will generate the same proportions from the compressively sensed data as from the traditionally sensed data. To see this, let \mathbf{P}^* denote the solution of (4). If \mathbf{Q} is any $M \times N$ proportion matrix, then $\|\mathbf{X}^{(c)} - \mathbf{E}^{(c)}\mathbf{Q}\|_2^2 = \|\mathbf{S}\mathbf{X}^{(u)} - \mathbf{S}\mathbf{E}^{(u)}\mathbf{Q}\|_2^2 = \|\mathbf{S}\|_2^2 \|\mathbf{X}^{(u)} - \mathbf{E}^{(u)}\mathbf{Q}\|_2^2$. Since \mathbf{S} is constant, the proportions that minimize the SSE in the compressively sensed domain must be the same proportions that minimize the SSE in the traditionally sensed domain.

The effects of noise on the proportions calculated by algorithm U may be different on compressively sensed data than on traditionally sensed data. The next section describes an empirical investigation that suggests the effect is not different. For this evaluation, SPICE is used for algorithm U [13].

Effect of Noise on Proportion Value Estimates The effect of noise on the estimate of proportion values computed from compressively sensed hyperspectral data was studied. To this end, zero-mean Gaussian noise was added to uncompressed simulated hyperspectral data. The data were simulated using ten endmembers selected from the ASTER Spectral Library, version 2.0. The endmembers used were Carbonate Burkeite, Chloride Carnallite, Sulfate Anhydrite, Dolomite, Phosphorite, Limestone, Basalt, Quartzite, Basanite, and Rhyolite. Simulated data were generated by sampling proportions from a uniform Dirichlet distribution and using them to form 2000 convex combinations of the endmembers. These spectra in the library ranged from $0.4\mu\text{m}$ to $2.5\mu\text{m}$. For this paper, every

3^{rd} wavelength was used resulting in $D = 351$. Gaussian noise was added to each simulated hyperspectral pixel. The noise levels were controlled by the standard deviations. The standard deviations σ were set to

$$\sigma = \frac{s \max\{\mathbf{X}^{(u)}\}}{100} \quad (5)$$

where $\max\{\mathbf{X}^{(u)}\}$ denotes the maximum value of the uncompressed data. Experiments were conducted for $s = 1, 2$ and 5 corresponding to 1%, 2% and 5% noise levels, respectively.

For each noise level and projection dimension $d \in \{20, 30, \dots, 351\}$, 10 sensing matrices S were sampled and used to compress noisy data. Each s_{ij} was sampled from a zero-mean, unit-variance Gaussian. For each S , estimates of the proportion matrix $\tilde{\mathbf{P}}$ were estimated from the noisy compressed and uncompressed data. The average error between the true proportions, \mathbf{P} , and the estimated proportions, $\tilde{\mathbf{P}}$, were computed as follows,

$$error = \frac{1}{MN} \sum_{i=1}^M \sum_{j=1}^N |\tilde{p}_{ij} - p_{ij}| \quad (6)$$

For each d , the mean and variance of the percentage errors associated with the 10 sensing matrices were calculated. An average signal to noise ratio was also calculated. Each time a noise value was sampled and added to an uncompressed spectral value, the ratio of the amplitude of the spectral value, A_s , to the noise value, A_n was used to calculate a signal-to-noise ratio, R , according to (7)

$$S = 20 \log_{10} \frac{A_s}{A_n}. \quad (7)$$

The plot in Figure (1) summarizes these statistics.

III. MEASURING PROPORTIONS USING COMPRESSIVE SENSING

In this section, a method of directly sensing the correct proportions using known endmembers is described. Let \mathbf{S} be a random $M \times D$ sensing matrix and define

$$\mathbf{A} \equiv (\mathbf{S}\mathbf{E}^{(u)})^{-1}\mathbf{S} \quad (8)$$

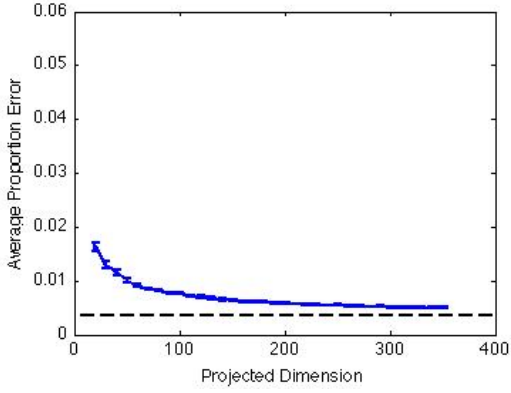
If $\mathbf{X}^{(u)} = \mathbf{E}^{(u)}\mathbf{P}$, then

$$\mathbf{A}\mathbf{X}^{(u)} = (\mathbf{S}\mathbf{E}^{(u)})^{-1}\mathbf{S}\mathbf{E}^{(u)}\mathbf{P} = \mathbf{P} \quad (9)$$

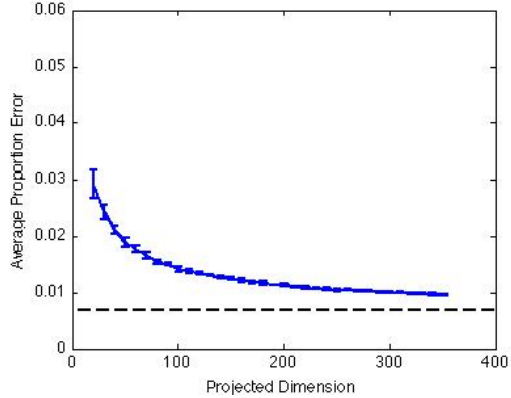
Therefore, using \mathbf{A} as the sensing matrix yields the proportions directly from the sensor. This is a remarkable and potentially extremely useful result.

IV. COMPUTING ENDMEMBERS AT LOW DIMENSIONS

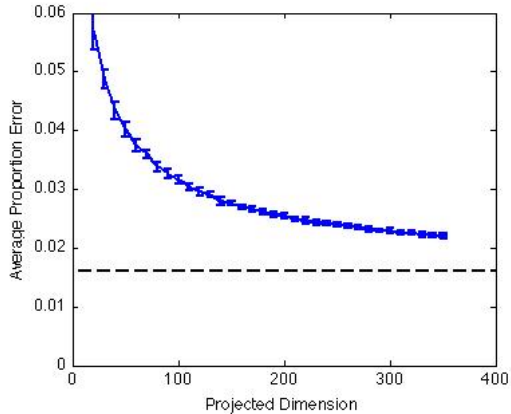
In this section, compressed endmembers are computed given the compressed data and the proportion values. When endmembers are unknown for a scene, the endmember estimation (described here) and the proportion estimation (described in Section II) steps can be combined to develop a spectral unmixing algorithm for compressed data without the need



(a) 1 % noise and mean signal-to-noise of 38dB



(b) 2 % noise and mean signal-to-noise of 32dB



(c) 5 % noise and mean signal-to-noise of 24dB

Fig. 1. Average error of estimated proportion values. The average error for the uncompressed noisy data with $\mathbf{S} = \mathbf{I}$ is represented by the dotted line. The results are found using an \mathbf{S} matrix composed of normally distributed sampled values. Error bars show one standard deviation across 10 random sensing matrices.

to decompress the measured spectra. The algorithm can proceed by alternating optimization between these two steps such as is done in the SPICE algorithm for uncompressed hyperspectral data [13]. If spectral information is of interest, then the endmembers can be reconstructed. There are only a few endmembers compared to the hundreds of thousands or millions of pixels.

Again for a given d , a random sensing matrix \mathbf{S} can be

generated and $\mathbf{X}^{(c)}$ can be computed. Recall that $\mathbf{X}^{(u)} = \mathbf{E}\mathbf{P}$. We also have the following uniqueness proposition.

Proposition IV.1. *If $\mathbf{X}^{(c)}$ can be expressed as a convex combination—using the same proportion matrix \mathbf{P} —of the column vectors of some matrix $\tilde{\mathbf{E}}^{(c)}$, i.e. $\mathbf{X}^{(c)} = \tilde{\mathbf{E}}^{(c)}\mathbf{P}$, then $\tilde{\mathbf{E}}^{(c)} = \mathbf{E}^{(c)} = \mathbf{S}\mathbf{E}^{(u)}$ for all matrix \mathbf{S} and for all low dimensional projections d , provided the number of pixels (N) is greater than the number of endmembers (M).*

The proof of this proposition is straightforward and is therefore omitted. As is the case for proportions, noise may mitigate the effectiveness of performing the calculations to estimate the endmembers directly on the compressively sensed data. Therefore, an empirical investigation was conducted.

Effect of noise on endmembers Zero-mean Gaussian noise was added to $\mathbf{X}^{(u)}$. The dimension d was varied from 20 to 351 with a step size of ten. For each value of d , one hundred sensing matrices \mathbf{S} were generated where each entry s_{ij} was sampled from a zero-mean, standard Gaussian. Each sensing matrix was used to compute a matrix of compressively sensed data $\tilde{\mathbf{X}}^{(c)}$. The noise level for the data was controlled by varying the standard deviation as per (5). For the given proportion matrix \mathbf{P} (i.e. the one that was used to generate $\mathbf{X}^{(u)}$), the compressed endmembers $\tilde{\mathbf{E}}^{(c)}$ were solved for by minimizing the least squares error. The solution for $\tilde{\mathbf{E}}^{(c)}$ is given by the following equation.

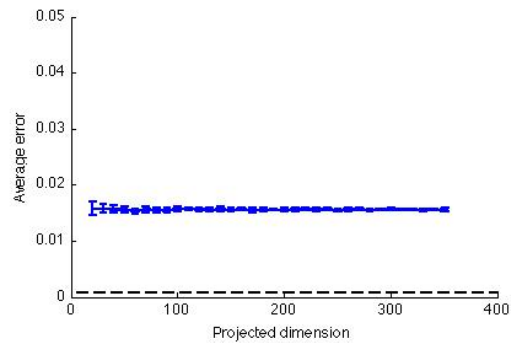
$$\tilde{\mathbf{E}}^{(c)} = \tilde{\mathbf{X}}^{(c)}\mathbf{P}^T (\mathbf{P}\mathbf{P}^T)^{-1} \quad (10)$$

This least squares solution $\tilde{\mathbf{E}}^{(c)}$ can be compared to $\mathbf{E}^{(c)}$ using the average error defined as in Eqs. (6). The average error was averaged over different random sensing matrices \mathbf{S} and for different values of d . The plots for 1%, 2%, and 5% noise levels are shown in Figure (2). As before, the mean signal-to-noise ratio is also computed. This error is computed over the estimated endmembers (whereas Figure (1) is computed over the estimated proportion values).

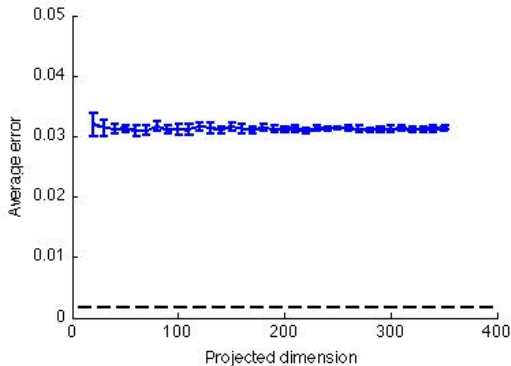
V. CONCLUSION AND FUTURE WORK

It has been shown that compressive sensing can be used to directly sense the proportions of materials present in a scene. In addition, a method to perform proportion estimation and endmember detection is developed for compressively sensed hyperspectral data. This method allows spectral unmixing to be performed directly on compressed data without any need to reconstruct hyperspectral imagery prior to analysis.

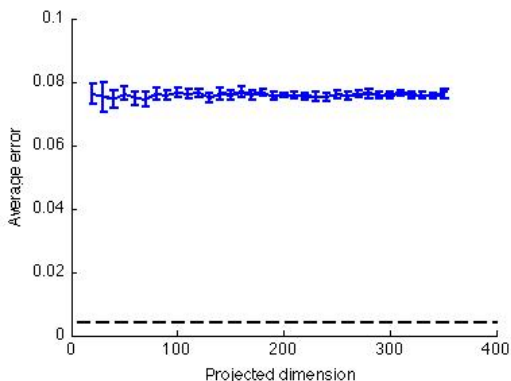
Results indicate that the error of estimate of the compressed endmembers is, on average, independent of the dimensionality of the compressed data. However, the variance of the percentage error increases with decreased compressed dimensionality. The error on the estimate of the proportions increases with decreased dimensionality in addition to an increase in the variance of the percentage error. This increased error in the proportion values may be due to the fact that the proportions are dependent and constrained to sum to one. Therefore, an error in one proportion value causes that another proportion value also be incorrect. The errors due to compression should be studied more, both empirically and analytically.



(a) 1 % noise and mean signal-to-noise of 38dB



(b) 2 % noise and mean signal-to-noise of 32dB



(c) 5 % noise and mean signal-to-noise of 24dB

Fig. 2. Average errors of estimated endmembers. The results are found using an \mathbf{S} matrix composed of normally distributed sampled values. Error bars show one standard deviation across 10 random sensing matrices.

Interesting future research activities include investigating methods for adaptively or non-adaptively optimizing sensing matrices for scenes, endmembers, and/or sensors building on ideas proposed in [14; 15] and also producing anomaly detection maps as direct outputs of the compressive imager.

REFERENCES

- [1] N. Keshava and J. F. Mustard, "Spectral unmixing," *IEEE Signal Processing Magazine*, vol. 19, pp. 44–57, 2002.
- [2] A. Zare and P. Gader, "Pcc: Piece-wise convex endmember detection," *IEEE Trans. on Geoscience and Remote Sensing*, vol. 48, no. 6, pp. 2620–2632, 2010.
- [3] N. Dobigeon, S. Moussaoui, M. Coulon, J. Tourneret, and A. O. Hero, "Joint Bayesian endmember extraction and linear unmixing for hyperspectral imagery," *IEEE Trans. Signal Processing*, vol. 57, no. 11, pp. 4355–4368, Nov. 2009.
- [4] J. Chanussot, M. M. Crawford, and B.-C. Kuo, "Foreword to the special issue on hyperspectral image and signal processing," *Geoscience and Remote Sensing, IEEE Transactions on*, vol. 48, no. 11, pp. 3871–3876, nov. 2010.
- [5] A. A. Green, M. Berman, P. Switzer, and M. D. Craig, "A transformation for ordering multispectral data in terms of image quality with implications for noise removal," *IEEE Trans. on Geoscience and Remote Sensing*, vol. 26, pp. 65–73, Jan. 1988.
- [6] A. Martinez-Uso, F. Pla, P. Garcia-Sevilla, and J. M. Sotoca, "Automatic band selection in multispectral images using mutual information-based clustering," in *Proceedings of the 11th Iberoamerican Congress on Pattern Recognition*, Cancun, Mexico, Nov. 2006, pp. 644–654.
- [7] J. B. Greer, "Sparse demixing," in *Proceedings of the SPIE*, vol. 7695, no. 769510, 2010.
- [8] M. Iordache, A. Plaza, and J. Bioucas-Dias, "Recent developments in sparse hyperspectral unmixing," in *Proceedings of the IEEE International Geoscience and Remote Sensing Symposium*, July 2010, pp. 1281–1284.
- [9] E. Candes, J. Romberg, and T. Tao, "Robust uncertainty principles: Exact signal reconstruction from highly incomplete frequency information," *IEEE Trans. on Information Theory*, vol. 52, no. 2, pp. 489–509, February 2006.
- [10] D. Donoho, "Compressed sensing," *IEEE Trans. on Information Theory*, vol. 52, no. 4, pp. 1289–1306, April 2006.
- [11] E. Candes and M. Wakin, "An introduction to compressive sampling," *IEEE Signal Processing Magazine*, vol. 25, no. 2, pp. 21–30, March 2008.
- [12] A. C. Gurbuz, J. H. McClellan, J. K. Romberg, and W. R. Scott, "Compressive sensing of parameterized shapes in images," in *ICASSP*, 2008, pp. 1949–1952.
- [13] A. Zare and P. Gader, "Sparsity promoting iterated constrained endmember detection for hyperspectral imagery," *IEEE Geoscience and Remote Sensing Letters*, vol. 4, no. 3, pp. 446–450, July 2007.
- [14] M. Elad, "Optimized projections for compressive sensing," *IEEE Trans. Signal Processing*, vol. 55, no. 12, pp. 5695–5702, December 2007.
- [15] J. M. Duarte-Carvajalino and G. Sapiro, "Learning to sense sparse signals: simultaneous sensing matrix and sparsifying dictionary optimization," *Trans. Img. Proc.*, vol. 18, pp. 1395–1408, July 2009.